

LRP 640/99

July 1999

**High growth rate deposition of hydrogenated
microcrystalline Silicon by a high current DC
discharge**

D. Franz, F. Grangeon, T. Delachaux,
A.A. Howling, Ch. Hollenstein

submitted for publication to
Applied Physics Letters

High Growth Rate Deposition of Hydrogenated Microcrystalline Silicon by a High Current DC Discharge

D. Franz, F. Grangeon, T. Delachaux, A. A. Howling, Ch. Hollenstein

Centre de Recherches en Physique des Plasmas,

Ecole Polytechnique Fédérale de Lausanne,

PPB Ecublens, CH-1015 Lausanne, Switzerland

J. Karner

Balzers AG, Balzers, Liechtenstein

Microcrystalline hydrogenated silicon films ($\mu\text{c-Si:H}$) have been deposited by a high current DC plasma in argon-silane-hydrogen mixtures at growth rates up to 10 nm/s and at substrate temperature below 500°C. Scanning electron microscopy, X-ray diffraction and FTIR analyses show that these films are highly crystallized. The obtained surface morphology depends strongly on the experimental conditions and varies from a cauliflower structure to a prismatic one. The crystalline orientation of the films also changes with the experimental conditions whereas some other properties such as crystallite size, columnar growth, and crystallinity of the films remain unchanged.

Fast deposition of hydrogenated microcrystalline silicon ($\mu\text{c-Si:H}$) films presents a great challenge for a large range of applications such as micro-electronic components and solar cell fabrication [1, 2]. Microcrystalline silicon exhibits important advantages compared to amorphous silicon (a-Si:H), such as higher electrical conductivity due to larger mobility. It is suitable for doped contact layers for solar cells and optical sensors. Moreover, it has a lower bandgap energy (1.1 eV) than the a-Si:H phase (1.7 eV) therefore allowing a better use of the solar spectrum in tandem solar cells [2]. Future industrial applications will require deposition processes with high growth rates at high devices quality. Until now, several authors have reported $\mu\text{c-Si:H}$ thin film deposition by RF plasma-enhanced CVD [3] or by hot-wire CVD [4] at growth rates up to 1 nm/s. Deposition of silicon thin films was also performed by cascaded arc plasma CVD at very high growth rates (up to 21 nm/s) but in this case, the films remained always amorphous [5]. The present letter deals with high growth rate deposition of $\mu\text{c-Si:H}$ by a low pressure, non-thermal DC plasma CVD [6].

The DC plasma CVD can be compared with the hot-wire CVD technique in which the filament is replaced by the hot plasma column. The main advantages of this new concept are the following : a higher temperature in the plasma is obtained, leading to a higher dissociation, to a higher radical production and to higher deposition rates. The reactor is easy to design and this new technique could lead to low contamination of deposited films since poisoning tungsten wire is replaced by the plasma column. Another advantage of the high current DC plasma reactor is that it is a powerful source for atomic hydrogen [6] which is known to be necessary for the deposition of $\mu\text{c-Si:H}$ [7]. The experimental set-up is shown in figure 1. A non-self-sustained DC discharge is maintained between a heated tungsten filament cathode and a water-cooled copper anode 50 cm apart. The current (I) can vary from 80 to 170 A and the discharge voltages are about 50 to 70 V. Results concerning the influence of the magnetic field on the film deposition will be published elsewhere. The stainless steel

vacuum chamber is evacuated by a roots pump and the working pressure is about 150 Pa. The process gases (argon, hydrogen, silane) are fed to the process chamber by mass flow controllers. The argon flux was kept constant at 1800 sccm. The hydrogen and silane fluxes were varied up to 200 sccm and 100 sccm respectively. The (100) silicon substrates are located around the discharge axis, at different distances from the center of the plasma column. The substrates have no active cooling or heating, their temperature is determined by the equilibrium between heating by atomic hydrogen recombination on the substrate surface, radiative and conduction losses. The substrate temperature is measured by a thermocouple fixed on the rear side of the sample. First, the substrates are heated by an argon-hydrogen plasma and when the temperature reaches the steady-state, silane gas is added to the discharge.

The film thickness was measured by in-situ laser interferometry and their results have been confirmed by SEM cross-section measurements. Depending strongly on experimental conditions, the growth rate of $\mu\text{c-Si:H}$ can be as high as 10 nm/s. On reducing the distance between the center of the plasma column and the substrate from 13 cm to 7 cm, the growth rate increases from 1.6 to 10 nm/s (see figure 2) while the temperature increases from 270°C to 450°C. This temperature rise is mainly due to a higher atomic hydrogen recombination rate at substrate surfaces nearer to the plasma column. A typical X-Ray Diffraction (XRD) patterns of the obtained films is presented in figure 3a. Peaks corresponding to the (111), (220) and (311) crystal planes of silicon are visible demonstrating that the films are highly crystallized. From the different diffraction patterns, it can be deduced that the crystal planes of the crystallites exhibit an orientation depending on the experimental conditions. The ratio of intensities of the diffraction peaks given by diffraction on crystalline silicon powder (no preferential orientation) is $I_{111}:I_{220}:I_{331} = 1:0.55:0.30$ [8]. In our case, the evolution of this ratio with experimental conditions indicates that the film orientation varies from a (220)

preferential orientation at high hydrogen flux or for substrates close to the plasma column, to a (111) preferential orientation in the case of a argon-silane plasma or at larger substrate-plasma distance (see fig. 2). The average crystallite size, calculated from the Scherrer formula [9] for the (111) and (220) diffraction peaks is about 12 (± 3) nm and depends weakly on experimental conditions. This crystal size is comparable to the one obtained in films deposited by the RF process [3]. Amorphous silicon films generally show a broad feature in the diffraction pattern around 27° (see figure 3b). For our films, no amorphous signature is visible in the diffraction patterns, i.e. the amorphous volume fraction in these films is extremely weak.

Figure 4a shows the SEM surface image of a microcrystalline silicon film deposited at a distance of 13 cm from the centre of the reactor. At this position, the deposition rate was about 1.6 nm/s, at a substrate temperature of about 370°C . The film shows clearly a cauliflower morphology. In figure 4b, the SEM image of a film surface produced nearer to the plasma (7 cm) with a deposition rate of 10 nm/s and substrate temperature about 450°C , shows a surface morphology with prismatic domains. These domains (cauliflower or pyramid) have an average size about 300 nm. It is interesting to note that the typical size of these domains is much greater than the average crystallite size obtained by XRD. This could be explained by a substructure of these domains, where the smallest structure are individual crystallites with a size as calculated from XRD patterns [10]. It should be noticed that, with except of the film orientation, the FTIR and XRD analysis show no noticeable differences in the physical properties of the films despite of their morphological difference. Figure 4c shows a SEM image of a film cross section in which the columnar structure of the film is clearly visible. The columns extend from the substrate to the film surface. No intermediate amorphous contact layer could be evidenced, in contrast to many other techniques [4]. The columnar film growth is explained by surface nucleation and a consequent shadowing effect

[11, 12]. Surface morphology and columnar structure are related since each surface domain (bulb or prismatic) is the top of a column. An attempt to explain the dependence of surface morphology on deposition conditions could be given by the Thornton model [13]. It is noticeable that the evolution of the surface morphology can be compared to the one deduced from structure zone models [13, 14]. The main parameter in these models is the surface temperature which can be related to the surface mobility. In our case, the evolution from a cauliflower to a prismatic morphology could be attributed to an increase of the surface mobility inducing a better surface crystallisation.

Figure 5 presents infrared absorption spectroscopy (FTIR) measurements in order to determine the hydrogen content and crystallinity of the film. The hydrogen content of the $\mu\text{-Si:H}$ films, deduced from the absorption peak at 615 cm^{-1} is less than 5% [15]. This value is close to the hydrogen content of $\mu\text{-Si:H}$ films produced by RF plasma-enhanced CVD at a deposition rate $<1\text{ nm/s}$, and compared to 15 % for a-Si:H films produced by the same technique [16]. Infrared absorption spectra (see figure 5) show very narrow absorption peaks at $615, 2080$ and 2100 cm^{-1} , whereas amorphous material exhibits broader absorption peaks, and a broad peak around 2000 cm^{-1} . Such absorption features were never observed in our samples. This last result is in good agreement with XRD observations, confirming the very low volume fraction of amorphous phase in our films.

It is important to note that we never obtained amorphous films in our deposition conditions, even in an argon-silane mixture without adding hydrogen. The films always present high crystallinity which seems to be quite independent of our experimental conditions. This is probably due to the high dissociative efficiency of the DC plasma process, meaning that in all used experimental conditions, the atomic hydrogen concentration is high enough to promote crystallisation of the layer. It is important to note that the films are not crystallized by

in-situ annealing : in our conditions, the substrate temperature ($<450^{\circ}\text{C}$) was substantially lower than the annealing temperature of about 600°C .

In conclusion, we have performed deposition of hydrogenated microcrystalline silicon thin films in a DC plasma reactor at deposition rates up to 10 nm/s and substrate temperature lower than 450°C . The films are well crystallized and exhibit a columnar growth. The surface morphology is strongly influenced by experimental conditions and changes from a cauliflower structure to a prismatic one. These results show that the DC plasma process can provide the high deposition rates necessary to make microcrystalline silicon an industrially interesting material. Further experiments will be performed in order to determine the porosity and the optical and electrical properties (defect density, dielectric constants,...) of these films.

This work was supported by the Swiss Priority Program for Materials.

Figure captions

Fig. 1 : Schematic side and cross-sectional representation of the DC reactor. Tr: cathode heating transformer, Ca: cathode, An: anode, PA: power supply, FC: mass flow controllers, S: substrate, P: plasma.

Fig. 2 : Evolution of the deposition rate and of the ratio of diffraction peaks with the substrate distance from the centre of the reactor (d).

Fig. 3 : Typical X-Ray Diffraction pattern of a) a $\mu\text{c-Si:H}$ produced by the DC plasma, and b) an a-Si:H thin film produced by a RF plasma. Both films are deposited on silicon substrates and have a thickness of about 1000 nm.

Fig. 4 : SEM images of $\mu\text{c-Si:H}$ thin films. a) cauliflower surface structure. b) prismatic surface structure. c) cross section of a $\mu\text{c-Si:H}$ thin film. The columnar structure of the layer is clearly visible.

Fig. 5 : Comparison of FTIR spectra of typical a-Si:H (produced by RF plasma) and $\mu\text{c-Si:H}$ (produced by DC plasma). Transmittance here is defined as the intensity transmitted by the coated substrate divided by that of the uncoated substrate.

Figures:

Figure 1 (D. Franz et al.):

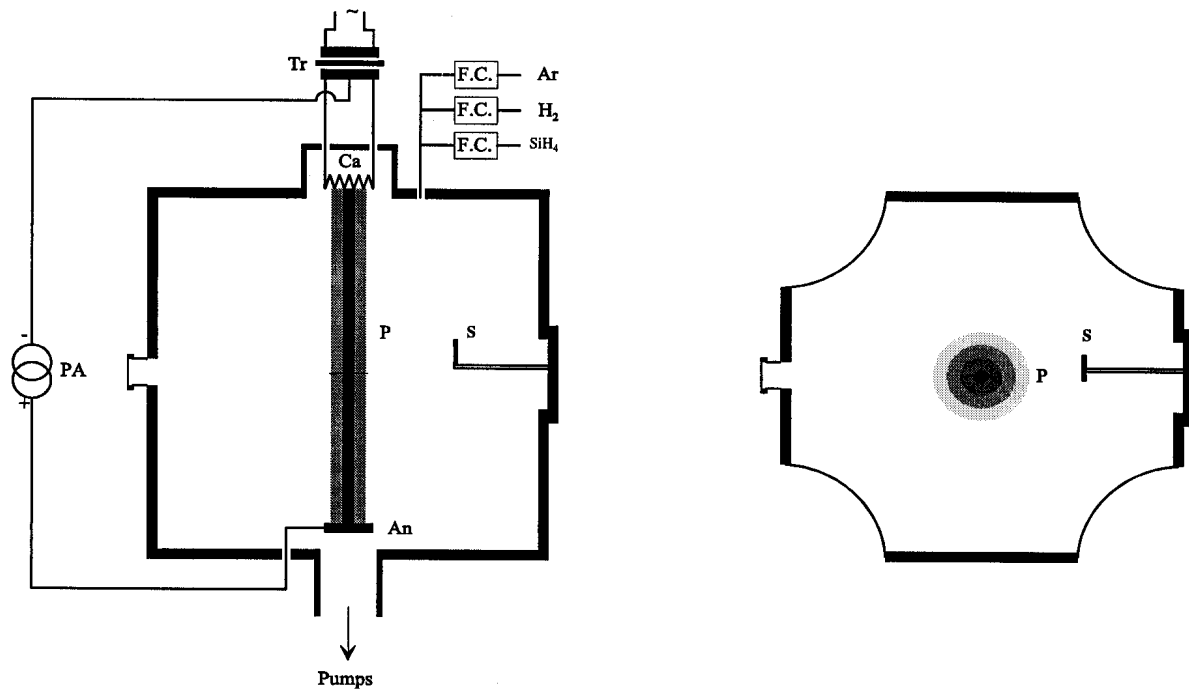


Figure 2 (D. Franz et al.):

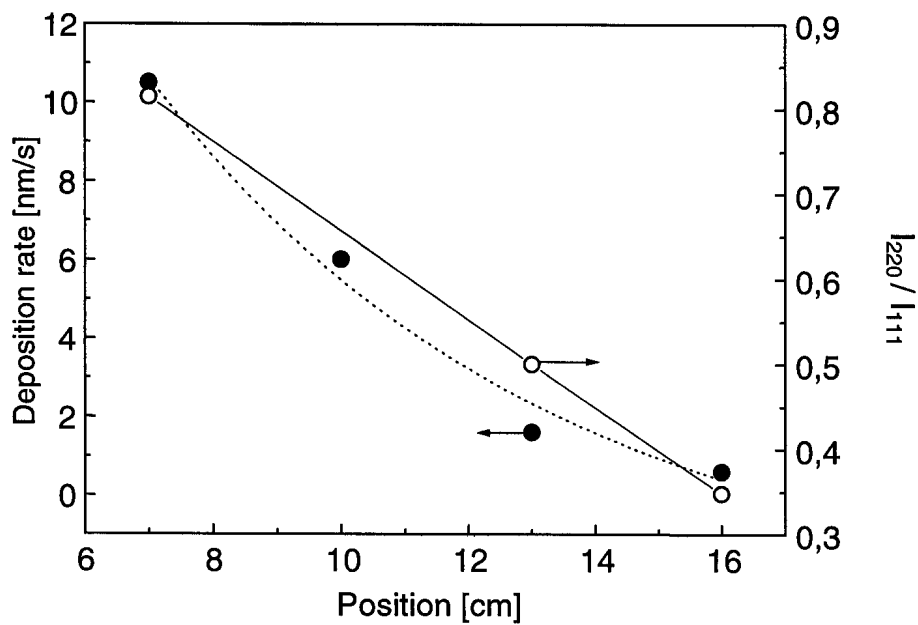


Figure 3 (D. Franz et al.):

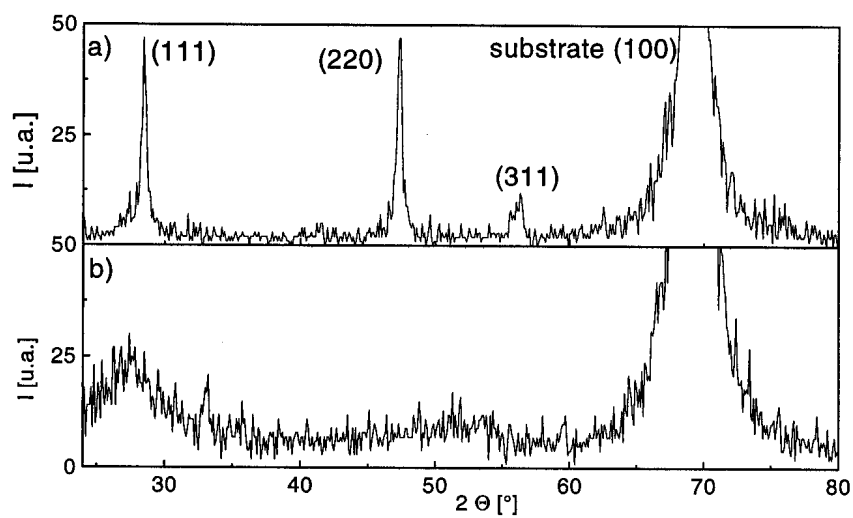


Figure 4 (D. Franz et al.):

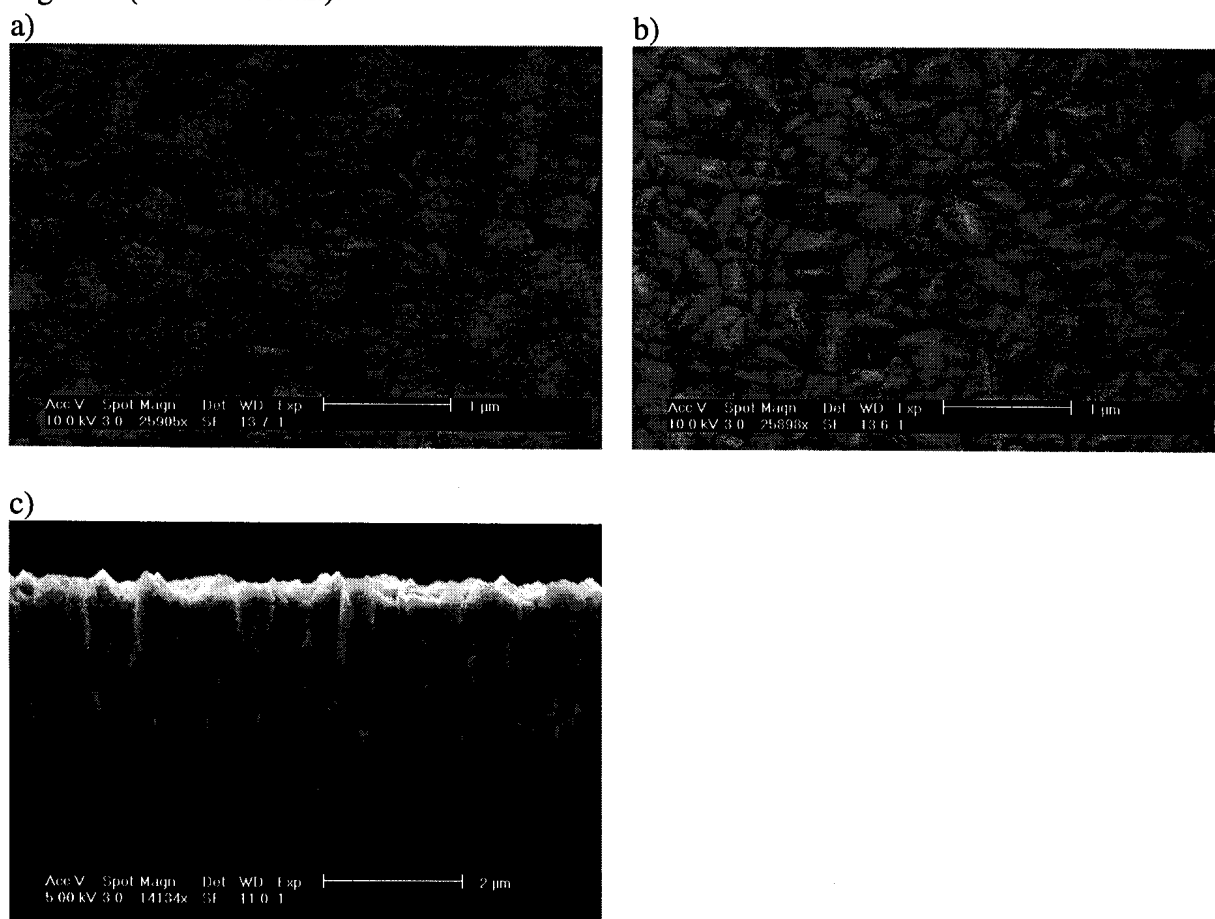
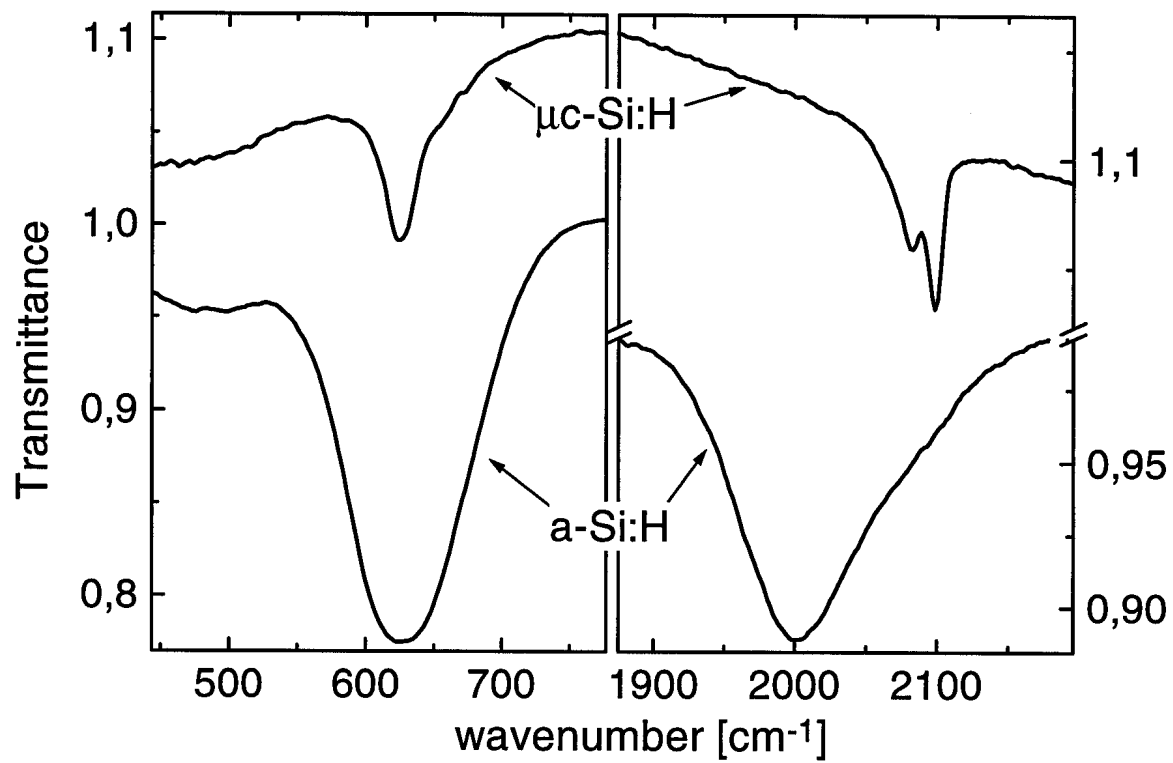


Figure 5 (D. Franz et al.):



References

- [1] A. Asano, *Appl. Phys. Lett.* **56** (1990) 533
- [2] S. Kumar, B. Drevillon and C. Godet, *J. Appl. Phys.* **60** (1986) 1542
- [3] U. Kroll, *J. Appl. Phys.* **80** (1996) 4971
- [4] J.K. Rath, H. Meiling and R.E.I. Schropp, *Jpn. J. Appl. Phys.* **36** (1997) 5436
- [5] W.M.M. Kessels, M.C.M. van de Sanden, R.J. Severens, L.J. van Ijzendoorn and D.C. Schram, *Mat. Res. Soc. Symp. Proc.* (1998) to be published
- [6] J. Karner, M. Peddrazini and C. Hollenstein, *Diamond and related materials*, **5** (1996) 217
- [7] C.C. Tsai, R. Thompson, C. Doland, F.A. Ponce, G.B. Anderson and B. Wacker, *Mater. Res. Soc. Symp. Proc.*, **118** (1988) 49
- [8] S. Yu, S. Deshpande, E. Gulari and J. Kanicki, *Mater. Res. Soc. Symp. Proc.*, **337** (1995) 69
- [9] H.P. Klug, *X-ray diffraction procedure* (John Wiley and Sons, New York, 1974)
- [10] E. Bardet, J.E. Bourée, M. Cuniot, J. Dixmier, P. Elkaim, J. Le Duigou, A.R. Middy and J. Perrin, *J. Non-Cryst. Solids* **198-200** (1996) 867
- [11] G.H. Gilmer and M.H. Grabow, *SPIE Vol. 821 Modeling of Optical Thin Films* (1987) 56
- [12] J.A. Thornton, *SPIE Vol. 821 Modeling of Optical Thin Films* (1987) 95
- [13] J.A. Thornton, *J. Vac. Sci. Technol.* **11**(1974)666
- [14] B.A. Movchan and A.V. Demchishin, *Phys. Met. Metallorg.* **28** (1969) 83

[15] M.H. Brodsky, Physical Review B, **16** (1977) 3556

[16] U. Kroll, J. Meier, A. Shah, S. Mikhailov and J. Weber, J. Appl. Phys. **80**
(1996) 4971